Supplementary Appendix

This appendix has been provided by the authors to give readers additional information about their work.

Supplement to: Mannstadt M, Harris M, Bravenboer B, et al. Germline mutations affecting Gα_{11} in hypoparathyroidism. N Engl J Med 2013;368:2532-4. DOI: 10.1056/NEJMc1300278

Supplementary Appendix

Germline Mutations Affecting $G\alpha_{11}$ in Hypoparathyroidism

Table of Contents

Supplemental description of the index cases and their families

Two Caucasian families with autosomal dominant isolated hypoparathyroidism were studied (see Fig. 1). The male index case of family A (subject 42, arrow in Fig. 1, left panel) was diagnosed at the age of 2 years with type 1 diabetes mellitus; at that time, total calcium level was within normal limits. At the age of 5 years he presented with generalized seizures, some of which were not associated with hypoglycemia; carbamazepine was given for 12 months and seizures did not re-occur after discontinuing this medication. At age 14 years, he complained of tremulousness and muscle cramps, and was found to be hypocalcemic with inappropriately low PTH levels. Review of the family history at that time revealed autosomal dominant transmission of hypocalcemia on his maternal side.

In family B, the index case (subject 21, arrow in Fig. 1, right panel) was diagnosed with isolated hypoparathyroidism when she presented with chronic fatigue and occasional muscle cramps at age 20; her laboratory evaluation revealed mild hypocalcemia and mild hyperphosphatemia with a low PTH level. Nine other family members were also diagnosed with isolated hypoparathyroidism; all had similarly mild symptoms of hypocalcemia.

None of the affected members in either family had a history of muco-cutaneous candidiasis, hearing loss, or renal abnormalities, and clinical examinations were unremarkable; in particular there was no evidence for skin changes.

Supplemental Methods

Consents and DNA collection

After obtaining written informed consent through our IRB approved protocol, blood samples were collected from affected and unaffected members of both families for DNA extraction using established methods.

Genetic Analysis

Sequence analysis of *CASR* was performed through the institutions of M.H. and B.B., respectively; *PTH* and *GCMB* were sequenced as described [1]. DNA samples from family A (3 healthy and 6 living affected) were genotyped using the InfiniumLinkage-24 SNP chip and multipoint linkage analysis was performed using GeneHunter [2,3]. For whole-exome sequencing, libraries were constructed with DNA from two affected members of each family (subjects 37 and

44 for family A; subjects 26 and 31 for family B) using the Agilent SureSelect Human All Exon Kit v2 [4] followed by massively parallel sequencing using an Illumina HiSeq Sequencer. Sequence data processing and variant calling was done using GATK [5] and annotation was performed using snpEff [6]; variants were considered to be potentially disease-causing when the allele frequency was ≤0.1% in 5,400 European control samples from the NHLBI Exome Sequencing Project (ESP), in dbSNP, and in the 1000 Genomes Project. PolyPhen2 was used to predict probably damaging rare missense, nonsense, or essential splice site variants. Identified mutations were confirmed by Sanger sequencing and restriction enzymatic digestion of PCR-amplified genomic DNA using the endonucleases Fsp1 and BsiEI, respectively.

Structural Analysis

Structural analyses and predictions are based on the crystal structure of a soluble, fully functional rat $G\alpha_{i/q}$ chimera, in which the N-terminal helix was replaced with that of mouse $G\alpha_{i1,}$ in complex with bovine $G\beta1/G\gamma2$ and the inhibitor YM-254890 (PDB ID 3AH8) [7]. Superposition with other heterotrimeric G protein complexes indicated that the chimeric substitution and inhibitor do not significantly alter the tertiary structure in the vicinity of the mutations. The mutations were modeled in the most common rotomer conformation compatible with the $G\alpha_{i/q}$ structure. Structural figures rendered with PyMOL [8] (DeLano Scientific LLC, Palo Alto, CA).

Table S1:
Diseases caused by somatic or germline mutations of guanine nucleotide-binding proteins

G protein	Mode of action	Disorders caused by somatic mutations	Mutation	Ref	Disorders caused by germline mutations	Mutation	Ref
$G\alpha_s$	activating	Pituitary adenomas, McCune-Albright Syndrome, and Fibrous Dysplasia	Arg^{201} Gln^{227}	9			
	activating/ LoF				Testotoxicosis/ Pseudohypoparathyroidism Neonatal diarrhea/ Pseudohypoparathyroidism	Ser^{366} $AVDT^{366-369}$ repeat	10 11
	inactivating or Δ methylation				Pseudohypoparathyroidism 1a or 1b	Multiple	12
$G\alpha_{t1}$	inactivating				Blindness (Nougaret)	Asp^{38}	13
$G\alpha_{t2}$	inactivating				Achromatopsia	Multiple	14
G_i	activating	Adrenocortical and ovarian tumors	Arg^{179}	9			
$G\alpha_q$	activating	Uveal Melanomas	Arg^{183} Gln^{209}	15	*Mouse dark skin**	Met^{179} Leu^{335}	16
$G\alpha_{11}$	activating	Uveal Melanomas	Arg^{183} Gln^{209}	17	*Mouse dark skin**	Ile^{63}	16
$G\alpha_{olf}$	inactivating				Primary Torsion Dystonia	Multiple	18

LoF; loss of function; *obtained through chemical mutagenesis in mice

Supplemental Figure 1:

Panel A: A genome-wide linkage scan for family A using all available members revealed a single linked region comprising approximately 10 Mb on chromosome 19p13.3 flanked by markers rs731714 and rs280521 (LOD score 3.0). Chromosomal location on the x-axis and parametric LOD score values on the y-axis.

Panel B: Nucleotide sequence analysis of *GNA11* exon 2 revealed a heterozygous nucleotide change, c.178C>T (p.Arg60Cys) for the index case 42 in family A (left panel). Nucleotide sequence analysis of *GNA11* exon 5 revealed a heterozygous nucleotide change, c.632C>G (p.Ser211Trp) for the index case 21 in family B (right panel).

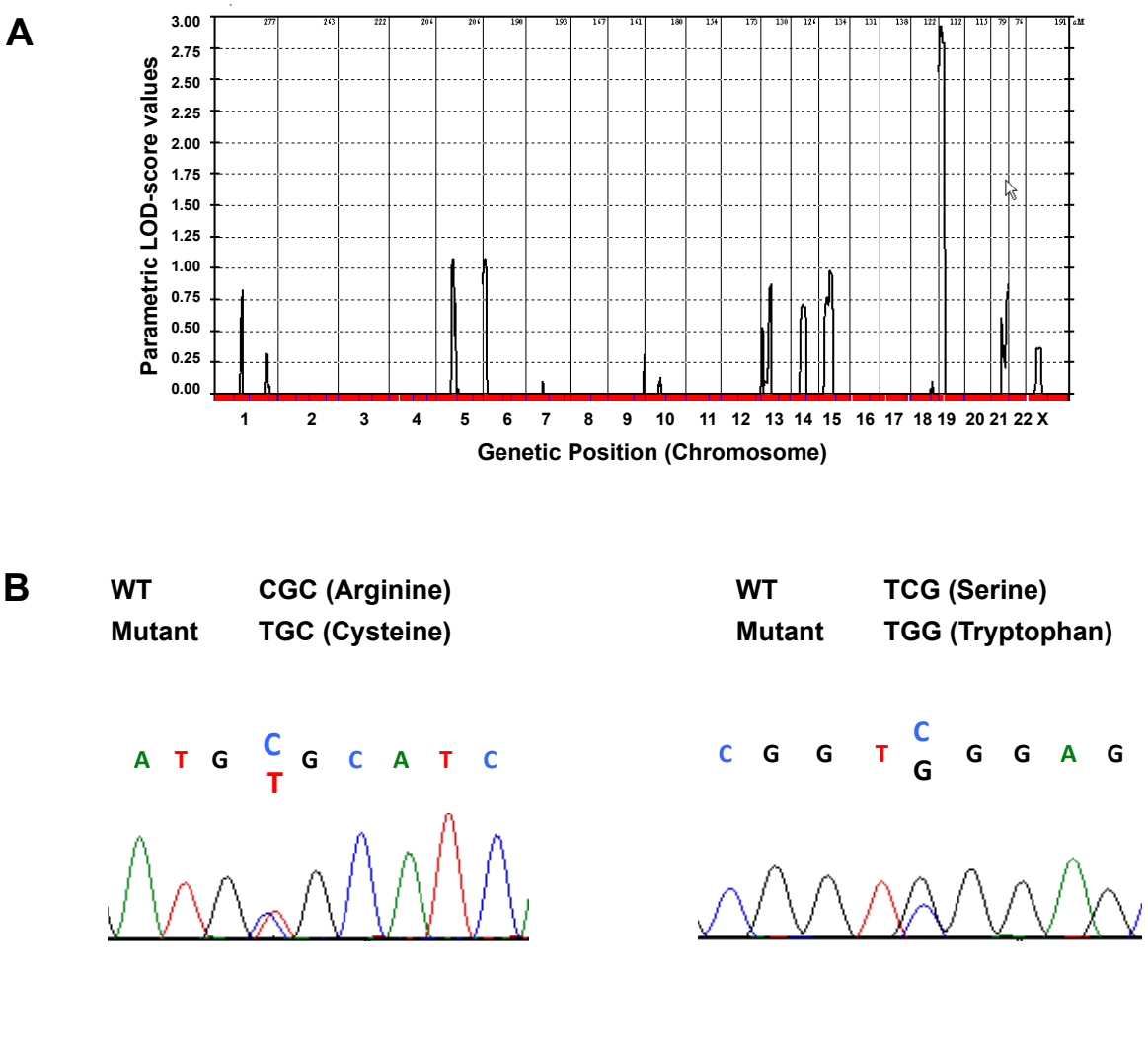

Supplemental Figure 2: Structural Analysis of Mutants

Model of $G\alpha_{11}$ based on the crystal structure of the $G\alpha_{i/q}\beta\gamma$ heterotrimeric complex (PDB ID 3AH8) [7]. Ribbon rendering shows the GTPase domain (green) and the helix αA (cyan).

Panel A: GDP, Arg60 and other relevant residues are shown as stick models [19]. Note polar interactions (magenta dashes) of Arg60 with Asp71 and the main chain carbonyl of Gly66, which likely stabilize the interaction of the helical with the GTPase domain. The polar interactions are disrupted by the cysteine substitution (right).

Panel B: Interaction of Ser211 (stick model) with the β-subunit (blue cartoon with semitransparent surface) is shown on the left. Substitution of Ser211 with tryptophan (spheres) is predicted to interrupt the interaction with βγ subunits (right).

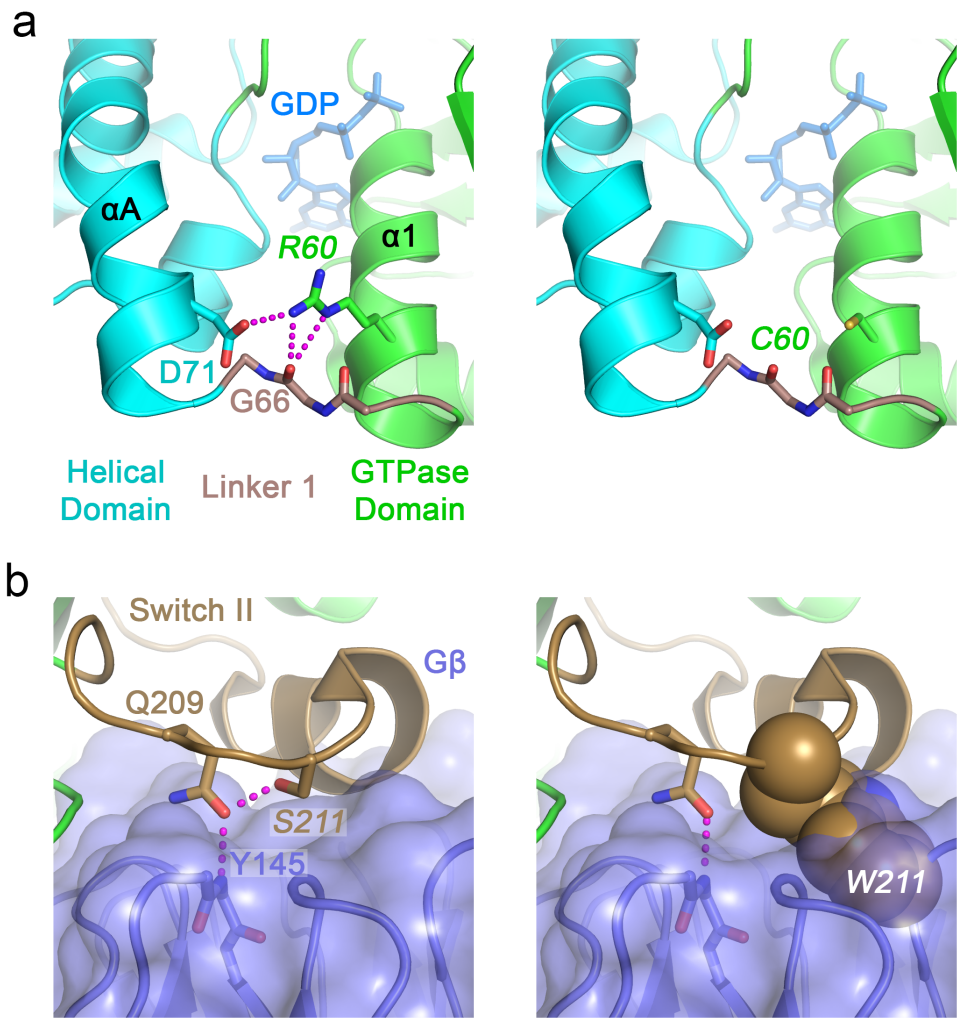

References

1. Mannstadt M, Bertrand G, Muresan M, et al. Dominant-negative GCMB mutations cause an autosomal dominant form of hypoparathyroidism. J Clin Endocrinol Metab 2008;93:3568-76.
2. Hoffmann K, Lindner TH. easyLINKAGE-Plus--automated linkage analyses using large-scale SNP data. Bioinformatics 2005;21:3565-7.
3. Kruglyak L, Daly MJ, Reeve-Daly MP, Lander ES. Parametric and nonparametric linkage analysis: a unified multipoint approach. Am J Hum Genet 1996;58:1347-63.
4. Gnirke A, Melnikov A, Maguire J, et al. Solution hybrid selection with ultra-long oligonucleotides for massively parallel targeted sequencing. Nat Biotechnol 2009;27:182-9.
5. DePristo MA, Banks E, Poplin R, et al. A framework for variation discovery and genotyping using next-generation DNA sequencing data. Nat Genet 2011;43:491-8.
6. Cingolani P, Platts A, Wang le L, et al. A program for annotating and predicting the effects of single nucleotide polymorphisms, SnpEff: SNPs in the genome of Drosophila melanogaster strain w1118; iso-2; iso-3. Fly 2012;6:80-92.
7. Nishimura A, Kitano K, Takasaki J, et al. Structural basis for the specific inhibition of heterotrimeric Gq protein by a small molecule. Proc Natl Acad Sci U S A 2010;107:13666-71.
8. Ordog R. PyDeT, a PyMOL plug-in for visualizing geometric concepts around proteins. Bioinformation 2008;2:346-7.
9. Farfel Z, Bourne HR, Iiri T. The expanding spectrum of G protein diseases. N Engl J Med 1999;340:1012-20.
10. Iiri T, Herzmark P, Nakamoto JM, van Dop C, Bourne HR. Rapid GDP release from Gs alpha in patients with gain and loss of endocrine function. Nature 1994;371:164-8.
11. Makita N, Sato J, Rondard P, et al. Human Gs alpha mutant causes pseudohypoparathyroidism type Ia/neonatal diarrhea, a potential cell-specific role of the palmitoylation cycle. Proc Natl Acad Sci U S A 2007;104:17424-9.
12. Bastepe M, Jüppner H. Pseudohypoparathyroidism, Albright's hereditary osteodystrophy, and progressive osseous heteroplasia: disorders caused by inactivating GNAS Mutations. In: DeGroot L, Jameson J, eds. Endocrinology. 6th ed. Philadelphia: W. B. Saunders Co.; 2010.
13. Dryja TP, Hahn LB, Reboul T, Arnaud B. Missense mutation in the gene encoding the alpha subunit of rod transducin in the Nougaret form of congenital stationary night blindness. Nat Genet 1996;13:358-60.
14. Kohl S, Baumann B, Rosenberg T, et al. Mutations in the cone photoreceptor G-protein alpha-subunit gene GNAT2 in patients with achromatopsia. Am J Hum Genet 2002;71:422-5.
15. Van Raamsdonk CD, Bezrookove V, Green G, et al. Frequent somatic mutations of GNAQ in uveal melanoma and blue naevi. Nature 2009;457:599-602.
16. Van Raamsdonk CD, Fitch KR, Fuchs H, de Angelis MH, Barsh GS. Effects of G-protein mutations on skin color. Nat Genet 2004;36:961-8.
17. Van Raamsdonk CD, Griewank KG, Crosby MB, et al. Mutations in GNA11 in uveal melanoma. N Engl J Med 2010;363:2191-9.
18. Fuchs T, Saunders-Pullman R, Masuho I, et al. Mutations in GNAL cause primary torsion dystonia. Nat Genet 2012;45:88-92.
19. Lambright DG, Noel JP, Hamm HE, Sigler PB. Structural determinants for activation of the alpha-subunit of a heterotrimeric G protein. Nature 1994;369:621-8.